

## Article

# Bio-Based Tannin Foams: Comparing Their Physical and Thermal Response to Polyurethane Foams in Lightweight Sandwich Panels

Marlon Bender Bueno Rodrigues <sup>1</sup>, Ronan Côrrea <sup>2</sup>, Pedro Henrique G. De Cademartori <sup>3</sup>, Ana C. R. Ribeiro <sup>4</sup>, Rodrigo Coldebella <sup>2</sup>, Rafael A. Delucis <sup>4</sup>, Nayara Lunkes <sup>4</sup> and André L. Missio <sup>4,\*</sup>

<sup>1</sup> Materials Engineering Undergraduate Course, Federal University of Pelotas (UFPel), Pelotas 96010-610, RS, Brazil; marlon.bender@ufpel.edu.br

<sup>2</sup> Graduate Program in Forestry Engineering (PPGEF), Federal University of Santa Maria (UFSM), Santa Maria 97105-900, RS, Brazil

<sup>3</sup> Graduate Program in Forestry Engineering (PPGEF), Federal University of Paraná, Curitiba 80210-170, PR, Brazil; pedroc@ufpr.br

<sup>4</sup> Graduate Program in Materials Science and Engineering (PPGCEM), Federal University of Pelotas (UFPel), Pelotas 96010-610, RS, Brazil; r.delucis@hotmail.com (R.A.D.)

\* Correspondence: andre.missio@ufpel.edu.br

**Abstract:** Rigid polyurethane foams are the better-performing material for the most common insulation purposes, like sandwich panels. Nevertheless, they are highly flammable materials, release toxic gases, and are manufactured from fossil sources. As an alternative, tannin foams are bio-based materials that work as innovative alternatives thanks to their great fire resistance, as well as lower smoke and harmful gases emissions. In the present study, lab-made foams of both materials were compared through morphology, thermal and fire degradation, mechanical properties, and water affinity in order to fill the technological gap between them and their related sandwich panels. It was observed that tannin foams are still relatively inhomogeneous (since formaldehyde was not used) and present a high affinity for water but have higher thermal and fire resistance. The flat compression strength of the polyurethane sandwiches was greater than that of tannin sandwiches (3.61 and 3.09 MPa, respectively) thanks, mainly, to the crosslinking degree difference between the resins. Also, tannin foams presented a lower weight loss (−70.684% lower weight loss in flammability tests than polyurethane foams) and the ability to self-extinguish the flame. Therefore, sandwich panels with tannin foam cores could be successful materials in areas that require protection against fire, such as the building engineering and automotive industries.

**Keywords:** fire resistance; natural polymer; biomass; tannic extract; MDF panel



**Citation:** Rodrigues, M.B.B.; Côrrea, R.; De Cademartori, P.H.G.; Ribeiro, A.C.R.; Coldebella, R.; Delucis, R.A.; Lunkes, N.; Missio, A.L. Bio-Based Tannin Foams: Comparing Their Physical and Thermal Response to Polyurethane Foams in Lightweight Sandwich Panels. *Compounds* **2024**, *4*, 1–16. <https://doi.org/10.3390/compounds4010001>

Academic Editor: Juan C. Mejuto

Received: 8 October 2023

Revised: 4 December 2023

Accepted: 15 December 2023

Published: 25 December 2023



**Copyright:** © 2023 by the authors. Licensee MDPI, Basel, Switzerland. This article is an open access article distributed under the terms and conditions of the Creative Commons Attribution (CC BY) license (<https://creativecommons.org/licenses/by/4.0/>).

## 1. Introduction

Polyurethane (PU) foams are the most versatile and well-performing material applied for insulation purposes—used mainly for walls and tubes—thanks to their low thermal conductivity [1,2] and low water absorption [3]. However, PUs are expensive and completely synthetic, and their performance is sensitive to high temperature and fire. These drawbacks have carried other solutions to the market, such as inorganic glass, rock wool, and also crops-based insulation mats of wood and straw, with special attention being paid to sulfur-free tannin foams [4], tannin foams reinforced with cellulose nanofibers [5,6], and bio-insulation material manufactured with geopolymers and wheat straw [7].

Even if these materials are well performing in many situations, they do not perform as well nor are they as versatile as PUs. For instance, rigid polyurethane foams are one of the most widely used and widespread core materials in the sandwich panel market due to their versatility, low density, good mechanical resistance, and ease of processing [8,9]. Indeed, polyurethane foams have the advantages of being lighter and more homogeneous,

which might not be always the case for other fibers. However, polyurethane foams are highly flammable synthetic materials with high smoke emissions which—when exposed to fire—emit toxic gases, such as carbon monoxide and hydrogen cyanide [10]. Usually, flame retardants that are used in these types of foam focus on the use of halogens, phosphorus, and nitrogen [11], although these have had harmful impacts on the biosphere [12]. PU foams possess a low limiting oxygen index (LOI) of ca. 19%, which explains the growing interest in modifying such materials to improve their flame-resistance properties. Ma et al. reported PU foam coatings based on phytic acid, flame-retardant copolymer (PVH), graphene oxide (GO), carbon nanotubes (CNTs), and boron nitride (BN), which were capable of self-extinguishing and possessed a high LOI (58.0 vol%) [13]. In another work, Wang et al. carried out a chemical incorporation of phosphophenanthrene and phosphate moieties into the structure of PU foams and detected a continuous flame-inhibition effect throughout the combustion of the polymer matrix [14]. Also, in this area of research, Tang et al. synthesized rigid PU foams from a phosphorized polyol with a total smoke production 49% lower than control samples, in addition to a peak heat release rate that was 40% lower [15]. Another disadvantage is that PU products are derived from oil, and with the increase in the price of petrochemical raw materials [16] coupled with the decrease in oil availability, this disadvantage is leading industries to find alternatives for sustainable products [17,18].

The core material is an important component of sandwich panels, as it plays crucial roles in the structural system. Therefore, new environmentally friendly products with properties equivalent to conventional foams are being developed and improved, as is the case with rigid foams based on tannin extract [19,20]. Tannin (TA) foams are innovative and natural polymeric materials obtained by copolymerizing the tannic extract with furfuryl alcohol in an acidic medium; this reaction allows for the expansion of the material which simultaneously cures with the evaporation of a low boiling solvent, resulting in a light and porous material [6,21]. The structure of this porous substance is completely composed of natural raw materials. The major component is condensed tannins, a plant product present in several plant species, obtained mainly from the bark of Acacia trees (*Acacia mearnsii*, *Acacia mollissima*) [22], while furfuryl alcohol is derived from furan obtained by the hydrolysis and dehydrogenation of sugars from different agricultural cultures [23].

Considering the bioeconomy issues, these phenolic foams have been tested and perfected by several researchers. Previous studies have proved the ability of these foams to match synthetic foams based on the positive characteristics of thermal insulation, low density, and reduced cost [24–26]. Unlike PU foams, the main advantage of TA foams is their exceptional fire-resistance characteristics, together with their low emission of smoke and harmful gases [27–29], which further reinforces the great potential of these foams in the replacement of conventional petrochemical foams in the most diverse applications, including sandwich panels. Li et al., for example, produced foams derived from tannin–furanic resins with distinct cellular/nonporous structures and registered an excellent thermal conductivity of 0.0239 W/m·K [30], while Li et al. found that increasing the larch tannin content (LT) in tannin rigid foams contributed to increases in the thermal conductivity from 0.03252 W/m·K (when the LT was 10%) up to 0.04345 W/m·K (when LT reached 30%) [31]. In another work, Yuan et al. proposed a steam-driven foaming mechanism to prepare TA rigid foams and reported that the steam-driven tannin–furanic-based foam showed excellent thermal conductivity (0.0286 W/m·K), considered by the authors to be ultra-low in comparison to the control TA foams produced in the same study [20].

In this sense, sandwich panels, with sustainable and fire-resistant foam cores, could be applied, for example, to building engineering, automotive industries, and the refrigeration and storage sectors. In the present study, we investigate the potential of rigid tannin foams in application as a core material in sandwich panels. We aim to compare lab-made foams of both tannin and polyurethane foams through morphology, mechanical properties, and water affinity, as well as thermal and fire degradation.

## 2. Materials and Methods

### 2.1. Raw Materials

To form the tannin-based natural foam, tannin extract from *Acacia mearnsii* De Wild was used, provided by Indústria SETA<sup>®</sup>. Furfuryl alcohol (98%), diethyl ether (99.9%), and sulfuric acid (95–98%), diluted to a concentration of 32%, were acquired from Sigma Aldrich (Burlington, MA, USA). The PU foam was produced from the combination of an already-prepared mixture of polyol (component A) and isocyanate (component B), purchased from the company Redelease<sup>®</sup>. According to the supplier, the polyol premix is composed of castor oil, crude glycerin oil, catalysts, and surfactants. The 3 mm-thick raw medium density fiberboard (MDF) sheets used on the faces of both panels were obtained from local businesses in the city of Santa Maria-RS.

### 2.2. Preparation of Foams and Sandwich Panels

The preparation of foams and sandwich panels is summarized in Figure 1. The rigid polyurethane foam was prepared by adding 90.8 g (52.5%) of isocyanate and 82.17 g (47.5%) of polyol, which were mixed with the aid of a drill, until the mixture resembled a cream. Afterwards, the mixture was placed in a 25 × 25 × 2.5 cm mold with an MDF bottom plate, and the chemical reactions were allowed to complete so that the excess foam could be removed. To assemble the sandwich panel, it was necessary to prepare a small amount of the mixture of isocyanate and polyol in the same proportions as above in order to adhere the foam to the MDF plate to the upper side

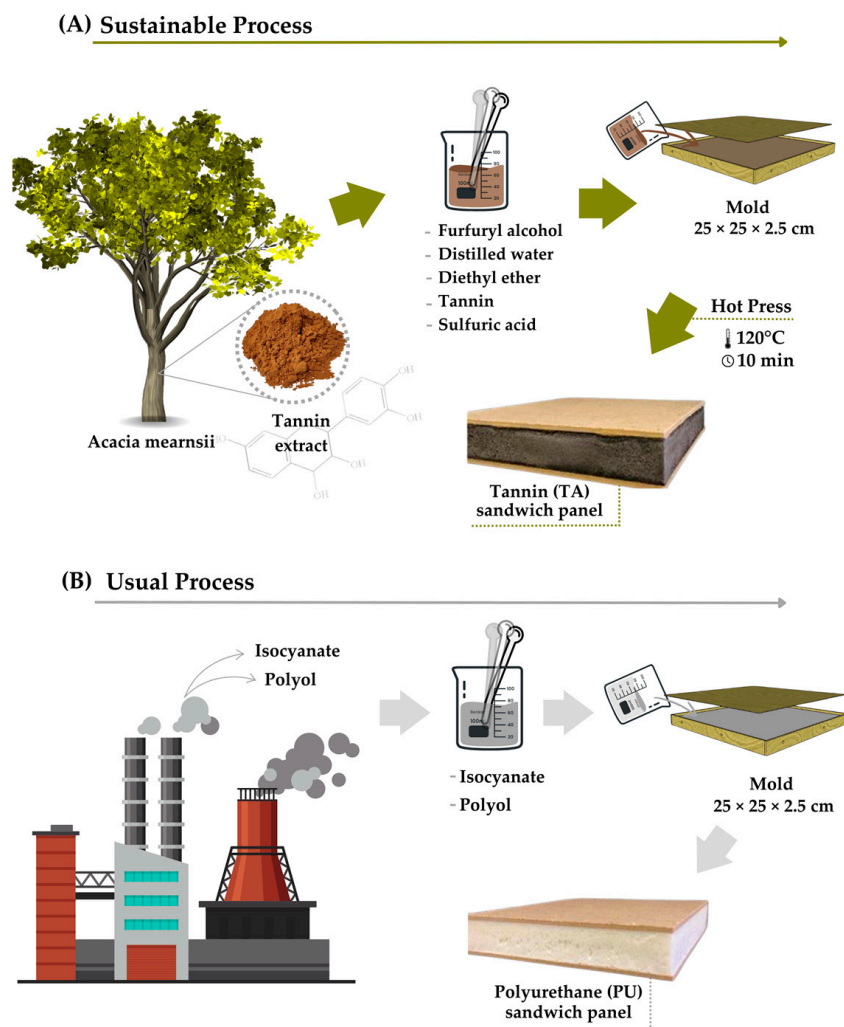


Figure 1. Experimental design of the production of the TA and PU sandwich panels.

The rigid tannin foams were prepared as follows: furfuryl alcohol (46.87 g), distilled water (46.87 g), and diethyl ether (9.37 g) were mixed with 187.5 g of tannin extract under manual agitation. After homogenization, 62.5 g of sulfuric acid (32% concentration) was added as a catalyst, and the mixture was homogenized for approximately 30 s. To make the panel, the mixture was placed in a 25 × 25 × 2.5 cm mold, with MDF sheets on both sides, and placed in a hydraulic press at 120 °C, without pressure for 10 min. Subsequently, the material was allowed to cool, and the edges of the mold were removed in order to obtain the sandwich panel.

### 2.3. Morphologic Investigation

The morphology of the foams was analyzed using a VEGA 3 scanning electron microscope (TESCAN, Czechia). Small cubes measuring 5 mm per side were cut and fixed in a metallic support before gold sputtering. The visualization was performed at 80, 200, 500, 1500, 6000, and 25,000 magnifications. ImageJ software (version 1.54f, National Institutes of Health, Bethesda, Rockville, MD, USA) was used to measure the average cell thickness and length through digital analysis of the SEM images. The cell dimensions were measured with over 100 readings for each sample. The average diameter was calculated using the empirical Equation (1) proposed by Tondi et al. [32].

$$Av.D = (\pi/4) \cdot D\bar{x}, \quad (1)$$

where D is the average diameter of the foams cells (μm) and  $D\bar{x}$  is the average of a hundred measured diameters (μm).

### 2.4. Flat and Lateral Compression Strength

The compressive strength of the TA and PU sandwich specimens was evaluated following the procedures of ASTM C365-16 for flat compression and ASTM C364-16 for lateral compression. Five replicates were evaluated for each type of material. The equipment used was an EMIC DL 2000 universal testing machine (INSTRON, São José dos Pinhais, Brazil), with a load capacity of 20 kN. For the flat compression tests, a load of 5 kN was applied at a speed of 0.25 mm/min, with a maximum deformation of 10%. Regarding the lateral compression test, a load of 5 kN was applied at a speed of 0.50 mm/min, with a maximum deformation of 10%.

### 2.5. Static Bending Test

Five specimens for each type of material underwent static bending in order to determine the strength and stiffness of the sandwich panels and the strength of the core. To carry out the test, the 3-point loading method was used, as described by the ASTM C393-16 standard. The equipment utilized was identical to that used for compression tests: an EMIC DL 2000 universal testing machine with a load capacity of 20 kN. A force of 5 kN was applied at a speed of 0.20 mm/min until the specimens ruptured.

### 2.6. Thermal Behavior

The TGA characterization was performed with the SDT Q600 thermogravimetric analyzer equipment (TA Instruments, New Castle, DE, USA). Samples of TA and PU foams of approximately 2 mg were heated from 30 °C to 1000 °C with a heating rate of 20 °C/min under an inert nitrogen atmosphere (gas flow 25 mL/min).

### 2.7. Direct Flame Exposition

For the determination of fire resistance, samples with 5 × 5 × 2.3 cm for foams and 5 × 5 × 3 cm for sandwich panels were exposed on their 5 × 5 side to the blue flame of a Bunsen burner at distance of 10 cm for 30 s for foams and 60 s for sandwich panels. When the samples ceased releasing smoke, the foams/panels were considered extinguished and

their masses were recorded to calculate the weight loss, according to Equation (2), as stated by Tondi et al. [33].

$$W = [(M_0 - M_1) \times 100] / M_0, \quad (2)$$

where  $W$  is the weight lost in the combustion (%),  $M_0$  is the initial sample mass (g),  $M_1$  is the final “post-combustion” sample mass (g).

### 2.8. Water Behavior

Five specimens for each material were exposed to water immersion for 2 and 24 h to determine their water absorption and thickness swelling. Specimens were cut into  $2 \times 2 \times 2 \text{ cm}^3$  cubes and dried overnight in an oven at  $60 \text{ }^\circ\text{C}$ . The specimens were immersed in distilled water at  $25 \text{ }^\circ\text{C}$ , removed at specific time intervals, and their surfaces were wiped. After, the samples were again weighed and measured at the end of the respective times.

### 2.9. Moisture Content and Apparent Density Determination

One of the most important parameters for porous materials is the density, and the normative method of ASTM D1622—14 was followed. Samples measuring approximately  $5 \times 5 \times 2.3 \text{ cm}$  for the foams and  $5 \times 5 \times 3 \text{ cm}$  for the sandwich panels were measured using five repetitions per material after stabilization at  $20 \text{ }^\circ\text{C}$  and 65% moisture content. The same samples were used to determine their equilibrium moisture content by drying them at  $103 \text{ }^\circ\text{C}$  until a constant mass was achieved.

### 2.10. Statistical Analysis

Thermal analyses were performed on one representative specimen for each material. The results were presented in the forms of graphs and/or tables, with means and standard deviation. The data obtained from each analysis were subjected to data normality and ANOVA tests. If the null hypothesis was rejected, significant differences were detected through Fisher’s least significant difference (LSD) test. All statistical analysis were conducted at a 95% confidence level.

## 3. Results and Discussions

The rigid tannin foams were formulated and developed aiming for a natural product; therefore, no formaldehyde chemical was used. The formulation was chosen through pre-evaluations, in which the best combination of constituents was subjected to tests. The bases for the evaluations were visual aspects of the mixture, as well as expansion and healing. Mixtures with large amounts of tannin extract were very viscous and, consequently, not homogeneous, which generated small portions of agglomerated particles, impairing the material formation process and resulting in a heavy and malformed foam. Mixtures with excess reagents, on the other hand, accelerated the reaction process, stimulating high expansion, large volumes of brittle foams, and empty cavities. For this reason, the ideal balance between components was sought, fixing the ratio of solids at 53% and liquids at 47%. The visual aspect of PU and tannin foams produced in the present study is reported in Figure 2.

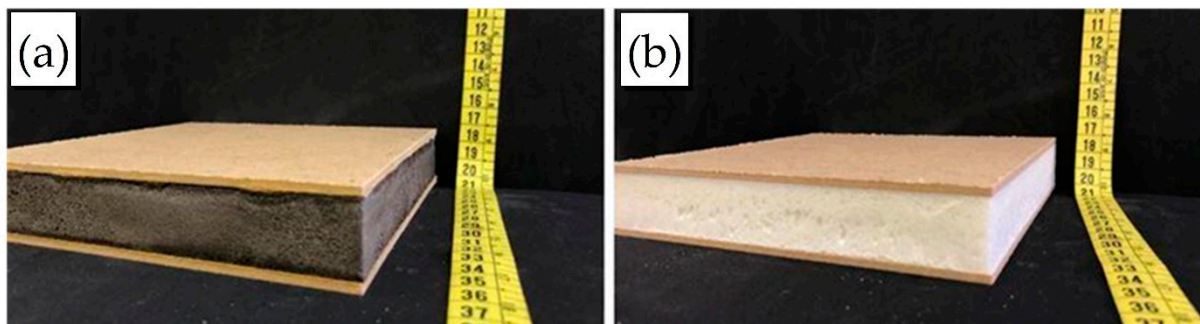


Figure 2. General aspects of sandwich panels: (a) TA rigid foam; (b) rigid PU foam.

### 3.1. Morphologic Investigation

Due to the different processes and chemistry of the PU and TA foams, the morphological properties of the produced foams were significantly different. Average cell diameter, length, thickness, and length/thickness ratio measurements are given in Table 1. Although significant differences for cell thickness and cell length were observed between the TA foam and the PU foam, the length/thickness ratio was statistically equal for the foams, mainly due to the high variability of the measurements for the TA foam, which is also correlated to its low homogeneity in cell shape.

**Table 1.** Morphological properties of the studied tannin and polyurethane foams. Different letters in the same column mean a statistical difference, at a 95% confidence level.

Material	Cell Thickness ( $\mu\text{m}$ )	Cell Length ( $\mu\text{m}$ )	Diameter ( $\mu\text{m}$ )	Length/Thickness
TA foam	$115.30 \pm 61.89$ a	$195.721 \pm 80.99$ a	121.26	$2.662 \pm 2.28$ a
PU foam	$215.21 \pm 49.02$ b	$350.795 \pm 41.82$ b	209.57	$1.726 \pm 0.53$ a

The morphology of tannin foams (Figure 3) reveals a brittle material in which cells are more irregular than the cells of PU foams. The high brittleness of the tannin-furanic foam is due to the high crosslinking degree of the furanic component [6]. The exponential speed of curing for these chemicals results in a less homogeneous cell structure that can be observed in the SEM images (red arrows in Figure 3a and red circle in Figure 3c). Furthermore, the content of closed cells appears to be lower than that of open cells. It is noteworthy that seemingly closed cells exhibit micropores in their structural walls (Figure 3d), which can be understood by other authors as indicating open cells [34]. Lacoste et al. produced TA foams filled with albumin and observed similar behaviors: a predominantly open-cell structure, with a small proportion of closed cells [35].

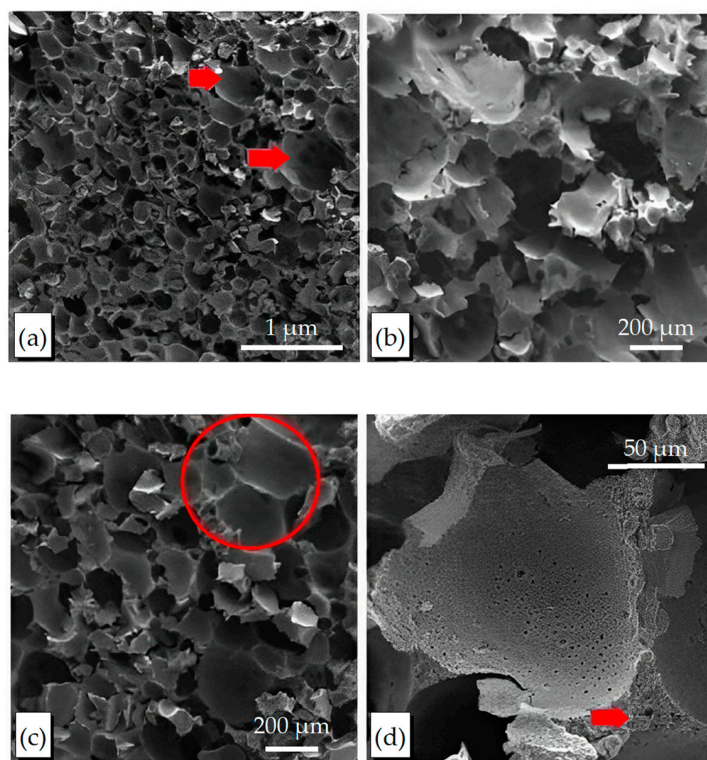


**Figure 3.** SEM high-resolution images of TA foams: (a) the middle of the panel, with the presence of voids, in the  $80\times$  magnification; (b) brittle structures, increase  $200\times$ ; (c) conserved dates cells, increase  $200\times$ ; (d) cell,  $1500\times$  magnification. Red circles and arrows in (a,c) indicate less homogeneous cell structure zones, while the red arrow in (d) indicates microvoids between the cells.

In the cellular structure images of the PU foam (Figure 4), there is an organized and homogeneous geometric arrangement of closed cells, displaying a strong interconnection between them (highlighted by the minuscule spaces between cells in Figure 4d), which play a crucial role in trapping the gas generated during the foam expansion process. The cell contours are clearly visible and defined, representing characteristic features of closed cells [2]. Conversely, Figure 4b reveals small holes present in the cell wall, which could lead to potential gas leakage and the ingress of liquids when exposed to conditions with high environmental moisture or liquid immersion. Similar structures have already been reported in the scientific literature: Delucis et al. researched the influence of different types of biomass (wood, tree bark, Kraft lignin, and paper sludge) on rigid PU foams, noting a closed cell content, on average, greater than 91% for all compositions produced [36].

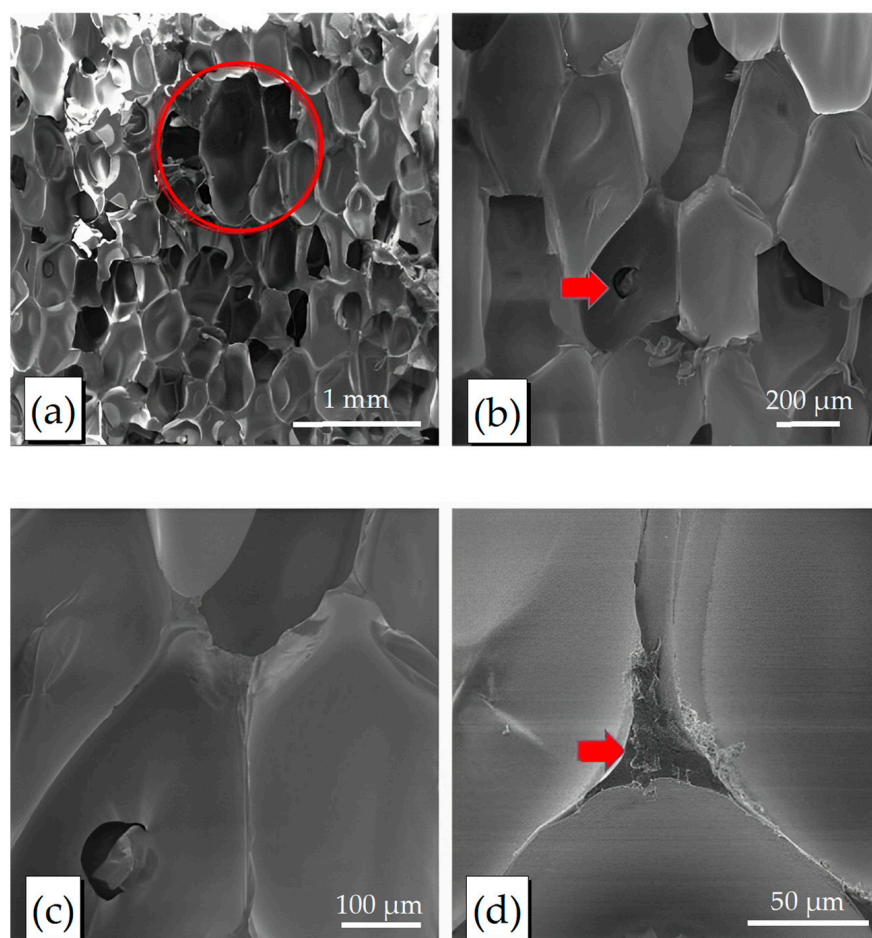


**Figure 4.** MEV images for PU foams: (a) empty space, 80× magnification; (b) perforated cell wall, 200× magnification; (c) increase of 500×; (d) connections between cells, increase of 1500×. The red circle in (a) indicates non homogeneous cell, the red arrow in (b) indicates a void in the cell wall, and the red arrow in (d) highlights the zone between cells.

In general, the morphological characteristics of TA foam differ from those of synthetic PU foam. The average diameter of PU foam cells is more than twice that of TA foam cells. Furthermore, the reason for the higher standard deviations observed for TA foams in Table 1 can be easily identified in the SEM images. This highlights a less homogeneous tannin foam. Some measures can be taken in order to improve the morphological characteristics of TA foams, such as: adapting and optimizing the foam formation process and making use of surfactants. Basso et al. [37] reported that incorporating a small proportion of nonionic surfactant leads to a more homogeneous cell size distribution.

### 3.2. Flat and Lateral Compression Strength

The compression test is one of the best methods to assess the maximum mechanical resistance of the sandwich panel core when subjected to an axial compressive force [38]. Table 2 presents the average values of both flat and lateral compression resistance of the sandwich panels.

**Table 2.** Average value of flat and lateral compressive strength for sandwich panels. Values followed by the same letter in the column do not show a statistically significant difference, at the 95% confidence level.

Material	Flat Compressive Strength (MPa)	Lateral Compression Strength (MPa)
TA sandwich	0.16 ± 0.01 a	3.09 ± 0.69 a
PU sandwich	0.27 ± 0.01 b	3.61 ± 0.02 a

As observed, the compression behavior can be attributed to the morphology exhibited by each foam. The TA foams display an irregular and fragile cellular structure with noticeable empty spaces (as depicted in Figure 3), characteristics that allow the cells to collapse more easily when force is applied to the material. A possible explanation for this is given by Tondi et al. [39], who assume that greater amounts of catalyst and furfuryl alcohol in the material formulation result in an excessively rigid polymer, consequently denser and more fragile. Another aspect to be considered is that the foams produced in this work are free of formaldehyde, due to this chemical product being highly toxic and carcinogenic [40]. Previous studies conducted by Tondi and Pizzi [32], in accordance with other authors [41,42], show that TA foam reinforced with formaldehyde exhibits improved material properties, especially in mechanics, demonstrating high compression resistance properties even surpassing those of synthetic PU foams. Link et al. [43] suggest that the use of formaldehyde is directly linked to the resin's crosslinking degree, wherein tannin/furfuryl alcohol polymers reinforced with formaldehyde are more likely to establish these crosslinks. This occurs due to methylol groups (methylated by formaldehyde) present in condensed tannins, allowing for the easier formation of covalent bonds with other flavonoid oligomers and/or with furfuryl alcohol. Hence, there is a necessity to discover an organic and health-friendly reinforcing agent that replaces the chemical formaldehyde while enhancing the overall properties of natural tannin foams [6]. Comparatively, PU foams exhibit greater resistance to compression owing to their homogeneous cellular structure, highly reticulated and with closed cells, enabling them to efficiently withstand applied force.

The lateral compression test was conducted to examine the behavior of the sandwich panels when subjected to the application of a force in the lateral direction of the plane, as well as to analyze potential failure modes that may result from this compressive load. Throughout the test, it was noted that both sandwich panels exhibited similar behavior. A noteworthy aspect to be considered when analyzing this property is the statistical equivalence between the two foams, which might be linked to a more significant impact of MDF plates on the lateral compression strength compared to the core of the sandwiches themselves. In the panel with TA foam, as the axial compression force was applied, the panel buckled, causing displacement of the upper sheet and rupture by cutting the core. A similar occurrence was noted for the PU sandwiches, albeit with a discrepancy in the level of displacement of the upper sheet. While for PU, the displacement was partial, for TA sandwiches the displacement was total. This type of displacement between the materials might have contributed to the slight difference in observed resistance and could be explained by the adhesive strength of the foams with the MDF plate.

During the process of expanding TA foam, as expansion occurs, a stiffer layer is formed on the foam's surface, being the first to polymerize and undergo the curing process [44]. Therefore, it is assumed that this characteristic might have influenced the adhesion of the porous material to the MDF plate, thereby reducing their affinity. Concerning the PU sandwiches, the procedure for manufacturing the panels differed, requiring the prepara-

tion of a small amount of isocyanate and polyol cream in the same proportions to bond the sheet to the foam. This process enhanced the adhesion between the materials since the stiffer layer—also formed by the synthetic foam—was removed due to the excess material produced.

### 3.3. Static Bending Test

The average values of modulus of elasticity and flexural strength of the TA and PU sandwich panels are shown in Figure 5. As observed in the graph, the values acquired from the static bending test indicate that, for flexural strength, panels with PU foam exhibited superiority to TA sandwiches, with a difference of approximately 32%. Conversely, the elastic modulus of the sandwich panels did not show a significant difference, according to the Fisher's LSD test.

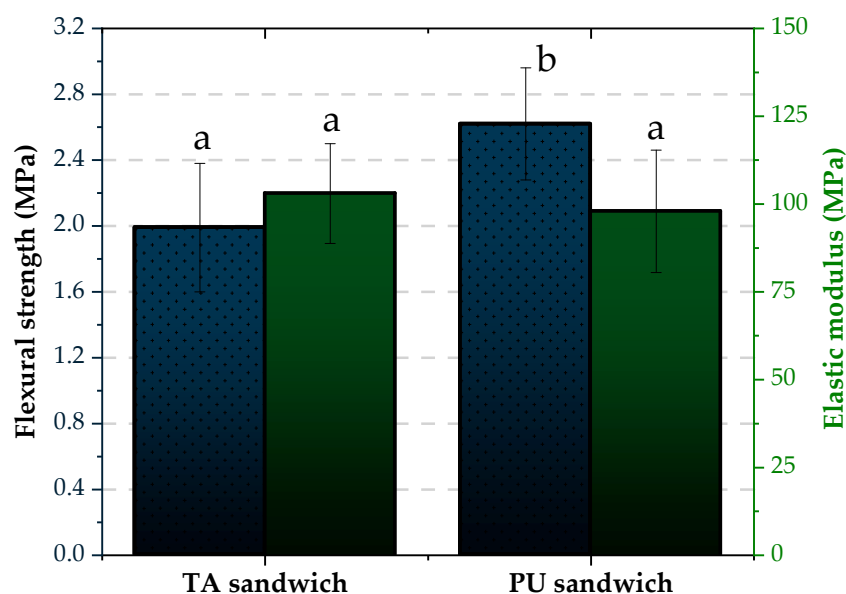


**Figure 5.** Flexural strength and elastic modulus of the obtained tannin and polyurethane sandwich panels. Values followed by the same letter do not show a statistically significant difference, at the 95% confidence level.

The inferiority demonstrated by the TA sandwich in static flexural properties is a consequence of the intrinsic characteristics of these foams, as discussed in the morphology section. As mentioned earlier, the absence of a reinforcing agent significantly influenced, primarily, the mechanical properties of the panels. Possibly, the rigidity and fragility of the cellular structure of the TA foams were responsible for the low mechanical resistance of the panels in compression and flexion modes. Regarding the elastic modulus, a possible explanation for the similarity of values between the sandwich panels is the influence of MDF plates, which—being materials of high rigidity and density—make the influence of foams on this specific property very low.

In general, irrespective of the foam type, the values obtained for the evaluated mechanical properties are lower than those mentioned in the literature by other authors, hindering comparison with other sources. A probable reason for this discrepancy was the utilization of an inappropriate load cell in the tests, as it was exerted excessive force beyond the materials' sensitivity, potentially distorting the actual values of the materials. However, given that the test conditions were identical for both samples, it is reasonable to conclude that the comparison between the recorded values confirms the higher flexural strength of the PU sandwich.

### 3.4. Thermal and Fire Behavior

The thermogravimetric analysis revealing the thermal degradation behavior of the produced materials is depicted in Figure 6. The TA foam shows a mild degradation—around 13%—until 300 °C, followed by a substantial material loss of approximately 60% of the mass until 550 °C. The initial mass loss event primarily results from moisture evaporation and partial degradation of low molecular weight compounds from tannin extract, such as simple sugars, phenol, and monomers [45]. Within the range of 300–500 °C, two main peaks of degradation are observed: the first at 442.20 °C and the other at 479 °C. These peaks correspond to the degradation of polyphenolic materials of the tannin extract [46], along with the breaking of C–C bonds and the complete breakdown of pyrolysis residual products from carbohydrates like glucose, mannose, and xylose [47,48]. As the material retains approximately 25% of its mass, it exhibits resistance to high temperatures and scarcely loses mass until 1000 °C. This remaining mass is a byproduct from the heat-induced polymerization of the foam, which limits the sample's pyrolysis [49].

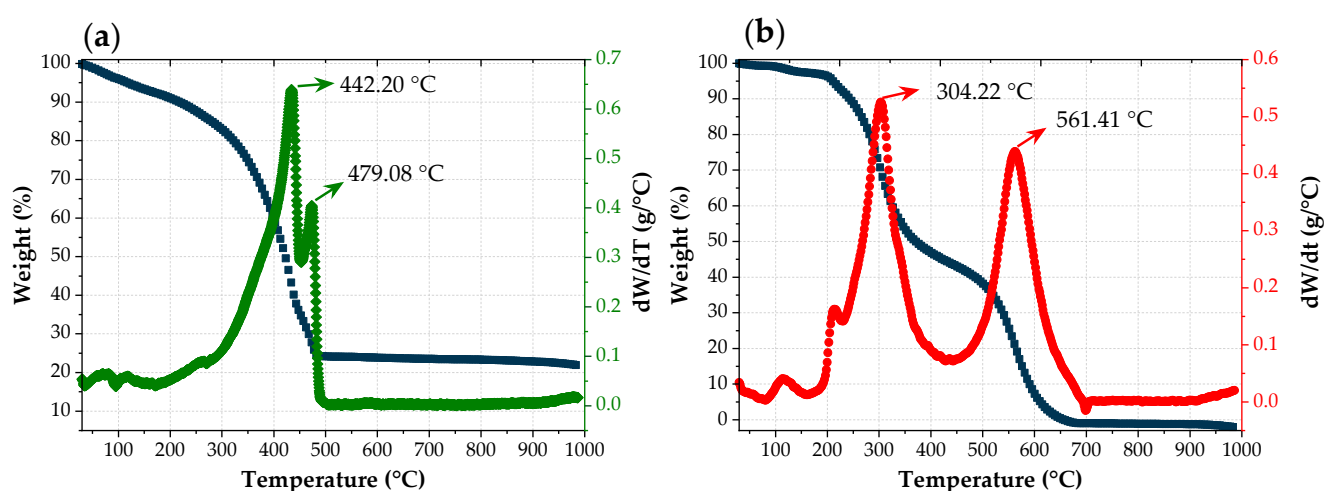


**Figure 6.** Thermogravimetric (TGA) curve and its derivative of (a) TA foam and (b) PU foam. The black lines represent the thermogravimetric curves, while the green line in (a) and the red line in (b) represent the first derivative of the TGA curve.

Figure 6b depicts that PU foam undergoes two primary thermal degradation events, with major peaks at 304.2 and 561.4 °C. The initial event may be attributed to the evaporation of unreacted isocyanate monomers from the foaming process [50] alongside decomposition reactions within urea and urethane groups, primarily occurring within side chains [36]. In the subsequent stage of decomposition, marked by the temperature peak at 561.4 °C, the pyrolysis of the condensed polyol is evident, a product originating from the initial degradation event of the polyurethane foam [51]. The resulting products from this degradation manifest as aliphatic ether alcohols and olefins, in addition to the generation of volatiles such as HCN and NO<sub>2</sub>, derived from amine groups and alkyl benzene originating from isocyanate groups [50]. Subsequently, the PU foam nearly completely loses its mass at 650 °C.

These results indicate that both polymers exhibit moderate heat resistance, with both experiencing significant degradation until 500 °C. At this point, the TA polymer stabilizes, whereas the PU degrades completely. This discrepancy has implications in the event of a fire, as the carbonized TA foam may retain some mechanical properties, while the PU foams completely collapse.

This behavior was also evident during direct flame exposure tests. In Figure 7, the weight loss and remains of the burned foams and sandwich panels after combustion are illustrated.

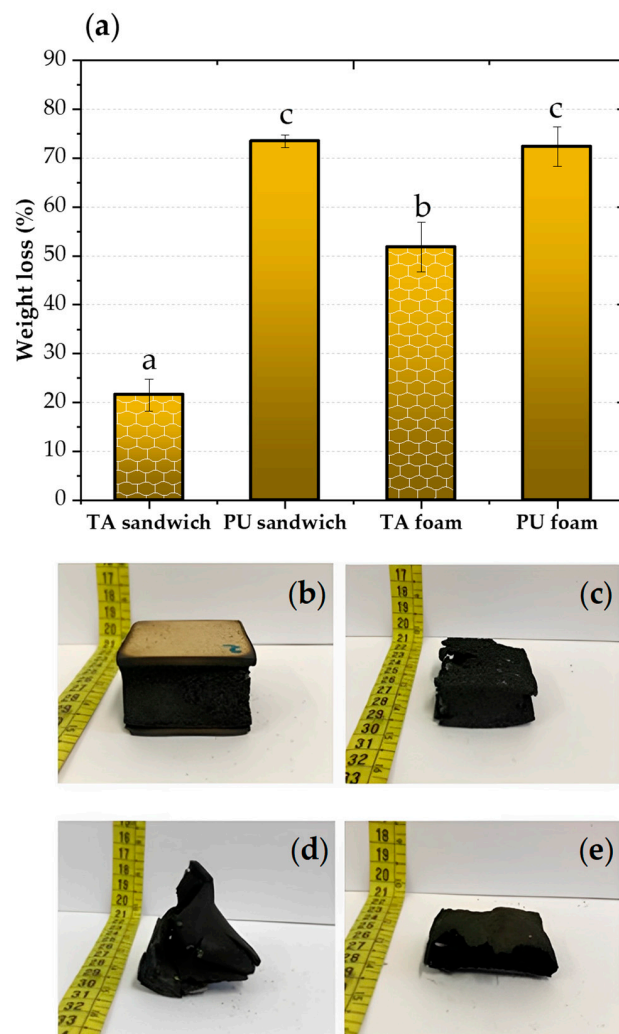


**Figure 7.** (a) Mean values of weight loss of TA and PU sandwiches/foams when exposed to fire and (b) TA sandwich, (c) TA foam, (d) PU sandwich, (e) PU foam after combustion. Values followed by the same letter in (a) do not show a statistically significant difference, at the 95% confidence level.

TA foams retained their shape when tested directly, and, even more interestingly, protected the back side of the panel, because of the self-extinguishable capability of tannin-furanic polymers. The PU foams and sandwich panels, on the other hand, were completely destroyed, losing both their mechanical and insulative properties. In Figure 7, the weight loss for the four specimens is reported to be numerical proof of the efficacy of tannin foams in fire suppression: the already significantly reduced weight loss registered by TA sandwiches (21.6%) becomes even more evident when the PU sandwiches are tested (73.5%). The high flammability of PU foams is often associated with their highly porous structure, responsible for facilitating the diffusion of oxygen within the polymeric foam matrix [52]. Furthermore, the low aromaticity contributes to rapid flame propagation in PU foams, as does its low limiting oxygen index (LOI) value of between 16% and 18% [53]. According to Fisher's LSD test, the weight loss values observed for the PU sandwich and the PU foam did not differ statistically.

The fire resistance exhibited by the TA foam is a consequence of the chemical structure of the cured resin, which is based on the various aromatic high-energy bonding rings. This structure carbonizes in contact with fire, creating a protective layer of carbon that prevents the flame from reaching the internal parts of the material [21]. Furthermore, the time until the self-extinguishing of the TA foam depends on several factors, including (i) the surface area that is reached by oxygen during the burning, (ii) the degree of polymerization of

the resin, and (iii) the cell wall thickness [54]. Thus, the morphology of TA foam, with a reduced cell diameter and thick cell wall, contributed to the foam self-extinguishing soon after the cessation of the fire.

An important factor to be mentioned is the observed difference in smoke emission during the analysis. PU foams have generated a substantial amount of smoke, and at the end of the test, the working environment (exhaust hood) was completely filled with smoke and soot. Conversely, this did not happen with TA foams, as their smoke emission was nearly negligible, almost zero.

### 3.5. Water Behavior and Apparent Density

The TA and PU foams and sandwich panels were immersed in water and their water absorption and thickness swelling were registered (Figure 8). The TA foams absorbed up to 3.5 times their weight when immersed in water for 24 h, while the PU foams exhibited lower absorption, ranging between 30 and 40% only. This is due to the morphology of the TA foams, but also to the hydroxy-rich nature of the phenolic-furanic polymer. This absorption proportionally affects the sandwich panels, even if the significantly higher weight of the panels mitigates the relative impact. Regarding the behavior of PU foams, the low water absorption is due to the partially closed cell structure and the hydrophobic nature of the material [55], potentially linked to the type of polyol used in its composition [56].

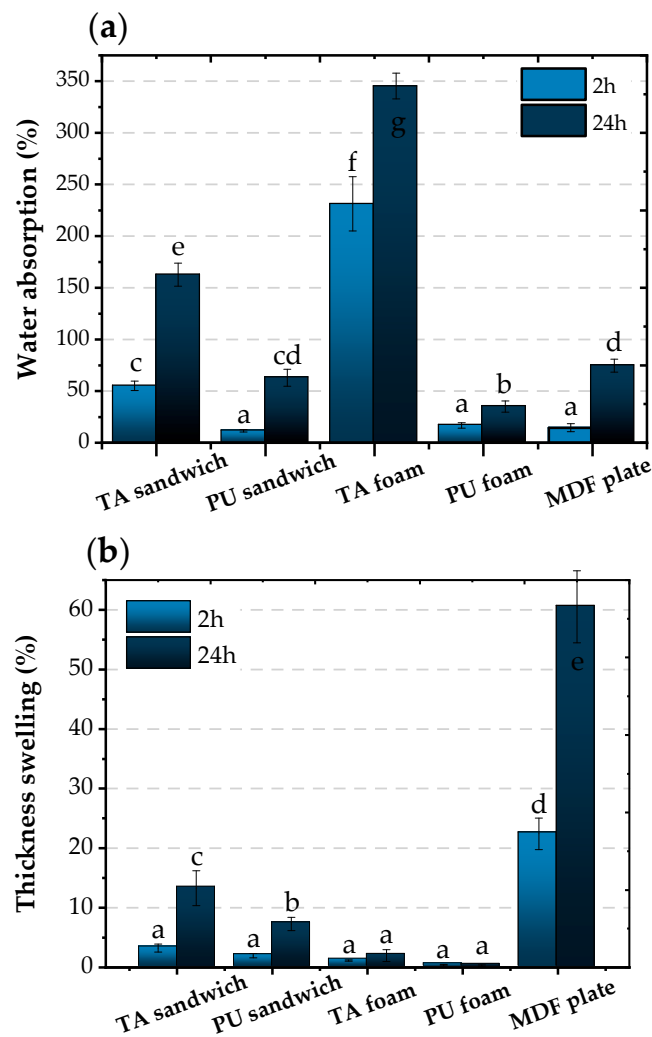


**Figure 8.** (a) Water absorption and (b) thickness swelling tests of the panels and their components in 2 h and 24 h. Values followed by the same letter in the graphs do not show a statistically significant difference, at the 95% confidence level.

Moreover, the evident difference in water absorption between the materials would, usually, suggest a proportional thickness swelling. However, due to the rigidity of the foam, they do not significantly modify their shape, being the higher impact on this phenomenon the MDF plates, which expand up to 60% of their thickness in 24 h immersion (Figure 8b). Additionally, it is noteworthy that the TA foams have considerable dimensional stability, since they have substantially absorbed more water (231.27%) compared to PU foams (16.84%), yet displaying low swelling, as previously noted by other researchers [54]. Concerning the MDF plate, the main contributing factor to the high swelling value in the panels was the cell wall of the lignocellulosic fibers composing the MDF. These cell walls swell until saturation, filling the empty spaces between the fiber bundles and increasing the thickness of the panel [57].

The average values of the moisture content of the sandwich panels and their components are shown in Table 3. The panels with a TA foam core exhibited a higher moisture content in comparison to the panels with PU foam. In the foams, the difference between the materials is more accentuated, with TA foams presenting a moisture content almost three times higher than that of PU foam. The average moisture content value for MDF plates was close to 8%, a value compliant with the criteria established by the Brazilian Association of the Wood Panel Industry for MDF panels [58]. According to Fisher's LSD test, foams and sandwich panels showed significantly equivalent moisture content values when the same core was used. In this sense, it is estimated that MDF plates did not have much influence on the moisture content of the TA sandwich and PU sandwich.

**Table 3.** Average values of moisture content and apparent density obtained for sandwich panels, foams and MDF plates conditioned at 20 °C and 65% humidity. Values followed by the same letter in the column do not show a statistically significant difference, at the 95% confidence level.

Material	Moisture Content (%)	Apparent Density (kg/m <sup>3</sup> )
TA sandwich	12.16 ± 0.22 b	298.78 ± 5.57 a
PU sandwich	6.52 ± 0.15 a	226.65 ± 8.10 b
TA foam	15.47 ± 0.52 b	127.86 ± 3.37 a
PU foam	5.55 ± 0.49 a	48.33 ± 2.47 b
MDF plates	7.99 ± 0.09 a	789.58 ± 4.88 c

Apparent densities of the produced materials are also presented in Table 3. The TA sandwiches exhibited approximately 32% more weight per unit area compared to the PU ones. A similar increase was observed for the foams, reaching a 165% increment. The higher weight in both TA foams and sandwiches can be attributed to several factors. Firstly, it is related to the amount of material required to fill a given volume. In the case of TA foams, almost twice as much material is needed compared to PU foams, owing to differences between the blowing processes. Another contributing factor that explains the higher density of TA foams is the use of additives or higher amounts of water in the formulation, responsible for producing denser foams and dissipating the heat generated during foam formation [33]. Conversely, an excess of furfuryl alcohol generates a greater amount of heat, inducing an accelerated cure, thus solidifying the mixture even before foam formation, consequently altering the final foam density [59]. At the same time, the higher moisture content in tannin-based foams might have contributed to the notable weight difference between the materials.

#### 4. Conclusions

Due to the process applied, the TA foams could not achieve the low densities, the small cell structures, and high homogeneity of the PU foams. On the other hand, due to their chemical nature, tannin foams showed a high fire resistance and water absorption. The excellent fire self-extinguishing properties of TA foam provided admirable protection to MDF boards when TA panels were directly exposed to flame, thus advocating for the

use of these innovative products when high fire resistance is required. This, coupled with a statistically equivalent lateral compression strength, implies potential applications of the produced sandwich panels in areas that require fire resistance, such as civil construction. However, the higher water affinity presents a drawback by potentially increasing the conductivity and moisture in specific applications, as insulation walls. Despite the good dimensional stability the TA sandwich exhibited, increased water absorption emerges as one of the most significant limitations for this sustainable material. In this sense, future research endeavors might address modifications in TA foam in order to mitigate this characteristic, explore sustainable chemicals and materials to enhance foam morphology and mechanical performance, and conduct comprehensive analyses of fire behavior, including with LOI, cone calorimeter, and thermal conductivity assessments.

**Author Contributions:** Conceptualization, R.C. (Ronan Côrrea) and A.L.M.; methodology, M.B.B.R., R.C. (Ronan Côrrea), N.L., and A.L.M.; formal analysis, M.B.B.R., R.C. (Ronan Côrrea), P.H.G.D.C., A.C.R.R. and R.C. (Rodrigo Coldebella); data curation, M.B.B.R., P.H.G.D.C., R.C. (Rodrigo Coldebella) and R.A.D.; writing—original draft preparation, M.B.B.R., R.C. (Ronan Côrrea), A.C.R.R., R.C. (Rodrigo Coldebella), R.A.D., N.L. and A.L.M.; visualization, M.B.B.R., P.H.G.D.C., R.A.D. and A.L.M.; supervision, P.H.G.D.C., R.A.D. and A.L.M.; Project administration, R.C. (Ronan Côrrea) and A.L.M.; funding acquisition, R.A.D. and A.L.M. All authors have read and agreed to the published version of the manuscript.

**Funding:** This research was funded by FAPERGS (Research Support Foundation of the State of RS): grant number 21/2551-0002243-4, the Technological Initiation and Innovation Scholarship (PROBITI-FAPERGS), and the Scientific Initiation Scholarship (PROBIC-FAPERGS) Institutional Programs. The authors are also indebted to CAPES (National Counsel of Technological and Scientific Development)—Finance Code 001, for the financial support given that allowed the development of the research.

**Data Availability Statement:** The study's data were presented in tables and figures, and, if desired, the data that support the findings of the manuscript can be obtained by contacting the corresponding author through a reasonable request.

**Acknowledgments:** The authors thank TANAC<sup>®</sup> industry for their donation of the tannic extract used in this research.

**Conflicts of Interest:** The authors declare no conflict of interest. The funders had no role in the design of the study; in the collection, analyses, or interpretation of data; in the writing of the manuscript; or in the decision to publish the results.

## References

1. Stanzone, M.; Oliviero, M.; Cocca, M.; Errico, M.E.; Gentile, G.; Avella, M.; Lavorgna, M.; Buonocore, G.G.; Verdolotti, L. Tuning of Polyurethane Foam Mechanical and Thermal Properties Using Ball-Milled Cellulose. *Carbohydr. Polym.* **2020**, *231*, 115772. [[CrossRef](#)] [[PubMed](#)]
2. Członka, S.; Sienkiewicz, N.; Kairyte, A.; Vaitkus, S. Colored Polyurethane Foams with Enhanced Mechanical and Thermal Properties. *Polym. Test.* **2019**, *78*, 105986. [[CrossRef](#)]
3. Dukarska, D.; Walkiewicz, J.; Derkowski, A.; Mirski, R. Properties of Rigid Polyurethane Foam Filled with Sawdust from Primary Wood Processing. *Materials* **2022**, *15*, 5361. [[CrossRef](#)] [[PubMed](#)]
4. Eckardt, J.; Neubauer, J.; Sepperer, T.; Donato, S.; Zanetti, M.; Cefarin, N.; Vaccari, L.; Lippert, M.; Wind, M.; Schnabel, T.; et al. Synthesis and Characterization of High-Performing Sulfur-Free Tannin Foams. *Polymers* **2020**, *12*, 564. [[CrossRef](#)] [[PubMed](#)]
5. Zhou, X.; Li, B.; Xu, Y.; Essawy, H.; Wu, Z.; Du, G. Tannin-Furanic Resin Foam Reinforced with Cellulose Nanofibers (CNF). *Ind. Crops Prod.* **2019**, *134*, 107–112. [[CrossRef](#)]
6. Missio, A.L.; Otoni, C.G.; Zhao, B.; Beaumont, M.; Khakalo, A.; Kämäräinen, T.; Silva, S.H.F.; Mattos, B.D.; Rojas, O.J. Nanocellulose Removes the Need for Chemical Crosslinking in Tannin-Based Rigid Foams and Enhances Their Strength and Fire Retardancy. *ACS Sustain. Chem. Eng.* **2022**, *10*, 10303–10310. [[CrossRef](#)] [[PubMed](#)]
7. Liu, L.; Zou, S.; Li, H.; Deng, L.; Bai, C.; Zhang, X.; Wang, S.; Li, N. Experimental Physical Properties of an Eco-Friendly Bio-Insulation Material Based on Wheat Straw for Buildings. *Energy Build.* **2019**, *201*, 19–36. [[CrossRef](#)]
8. Ates, M.; Karadag, S.; Eker, A.A.; Eker, B. Polyurethane Foam Materials and Their Industrial Applications. *Polym. Int.* **2022**, *71*, 1157–1163. [[CrossRef](#)]
9. Eling, B.; Tomović, Ž.; Schädler, V. Current and Future Trends in Polyurethanes: An Industrial Perspective. *Macromol. Chem. Phys.* **2020**, *221*, 2000114. [[CrossRef](#)]

10. Ciecierska, E.; Jurczyk-Kowalska, M.; Bazarnik, P.; Kowalski, M.; Krauze, S.; Lewandowska, M. The Influence of Carbon Fillers on the Thermal Properties of Polyurethane Foam. *J. Therm. Anal. Calorim.* **2016**, *123*, 283–291. [[CrossRef](#)]
11. Zhu, M.; Ma, Z.; Liu, L.; Zhang, J.; Huo, S.; Song, P. Recent Advances in Fire-Retardant Rigid Polyurethane Foam. *J. Mater. Sci. Technol.* **2022**, *112*, 315–328. [[CrossRef](#)]
12. Yin, Z.; Lu, J.; Hong, N.; Cheng, W.; Jia, P.; Wang, H.; Hu, W.; Wang, B.; Song, L.; Hu, Y. Functionalizing  $Ti_3C_2T_x$  for Enhancing Fire Resistance and Reducing Toxic Gases of Flexible Polyurethane Foam Composites with Reinforced Mechanical Properties. *J. Colloid Interface Sci.* **2022**, *607*, 1300–1312. [[CrossRef](#)] [[PubMed](#)]
13. Ma, Z.; Zhang, J.; Liu, L.; Zheng, H.; Dai, J.; Tang, L.-C.; Song, P. A Highly Fire-Retardant Rigid Polyurethane Foam Capable of Fire-Warning. *Compos. Commun.* **2022**, *29*, 101046. [[CrossRef](#)]
14. Wang, J.; Xu, B.; Wang, X.; Liu, Y. A Phosphorous-Based Bi-Functional Flame Retardant for Rigid Polyurethane Foam. *Polym. Degrad. Stab.* **2021**, *186*, 109516. [[CrossRef](#)]
15. Tang, G.; Liu, M.; Deng, D.; Zhao, R.; Liu, X.; Yang, Y.; Yang, S.; Liu, X. Phosphorus-Containing Soybean Oil-Derived Polyols for Flame-Retardant and Smoke-Suppressant Rigid Polyurethane Foams. *Polym. Degrad. Stab.* **2021**, *191*, 109701. [[CrossRef](#)]
16. Kilian, L.; Zhou, X. The Impact of Rising Oil Prices on U.S. Inflation and Inflation Expectations in 2020–23. *Energy Econ.* **2022**, *113*, 106228. [[CrossRef](#)]
17. Pawlik, H.; Prociak, A. Influence of Palm Oil-Based Polyol on the Properties of Flexible Polyurethane Foams. *J. Polym. Environ.* **2012**, *20*, 438–445. [[CrossRef](#)]
18. Zhang, Y.; Duan, C.; Bokka, S.K.; He, Z.; Ni, Y. Molded Fiber and Pulp Products as Green and Sustainable Alternatives to Plastics: A Mini Review. *J. Bioresour. Bioprod.* **2022**, *7*, 14–25. [[CrossRef](#)]
19. Eckardt, J.; Sepperer, T.; Cesprini, E.; Šket, P.; Tondi, G. Comparing Condensed and Hydrolysable Tannins for Mechanical Foaming of Furanic Foams: Synthesis and Characterization. *Molecules* **2023**, *28*, 2799. [[CrossRef](#)]
20. Yuan, W.; Xi, X.; Zhang, J.; Pizzi, A.; Essawy, H.; Du, G.; Zhou, X.; Chen, X. A Novel Strategy Inspired by Steaming Chinese Steamed Bread for Preparation of Tannin-Furanic Rigid Bio-Foam. *Constr. Build. Mater.* **2023**, *376*, 131035. [[CrossRef](#)]
21. Tondi, G.; Fierro, V.; Pizzi, A.; Celzard, A. Tannin-Based Carbon Foams. *Carbon N. Y.* **2009**, *47*, 1480–1492. [[CrossRef](#)]
22. Missio, A.L.; Tischer, B.; dos Santos, P.S.B.; Codevilla, C.; de Menezes, C.R.; Barin, J.S.; Haselein, C.R.; Labidi, J.; Gatto, D.A.; Petutschnigg, A.; et al. Analytical Characterization of Purified Mimosa (*Acacia mearnsii*) Industrial Tannin Extract: Single and Sequential Fractionation. *Sep. Purif. Technol.* **2017**, *186*, 218–225. [[CrossRef](#)]
23. Yang, T.; Ma, E.; Cao, J. Synergistic Effects of Partial Hemicellulose Removal and Furfurylation on Improving the Dimensional Stability of Poplar Wood Tested under Dynamic Condition. *Ind. Crops Prod.* **2019**, *139*, 111550. [[CrossRef](#)]
24. Pizzi, A.; Tondi, G.; Pasch, H.; Celzard, A. Matrix-assisted Laser Desorption/Ionization Time-of-flight Structure Determination of Complex Thermoset Networks: Polyflavonoid Tannin–Furanic Rigid Foams. *J. Appl. Polym. Sci.* **2008**, *110*, 1451–1456. [[CrossRef](#)]
25. Basso, M.C.; Li, X.; Fierro, V.; Pizzi, A.; Giovando, S.; Celzard, A. Green, Formaldehyde-Free, Foams for Thermal Insulation. *Adv. Mater. Lett.* **2011**, *2*, 378–382. [[CrossRef](#)]
26. Borrero-López, A.M.; Nicolas, V.; Marie, Z.; Celzard, A.; Fierro, V. A Review of Rigid Polymeric Cellular Foams and Their Greener Tannin-Based Alternatives. *Polymers* **2022**, *14*, 3974. [[CrossRef](#)]
27. Chen, X.; Li, J.; Essawy, H.; Pizzi, A.; Fredon, E.; Gerardin, C.; Du, G.; Zhou, X. Flame-Retardant and Thermally-Insulating Tannin and Soybean Protein Isolate (SPI) Based Foams for Potential Applications in Building Materials. *Constr. Build. Mater.* **2022**, *315*, 125711. [[CrossRef](#)]
28. Chen, X.; Li, J.; Pizzi, A.; Fredon, E.; Gerardin, C.; Zhou, X.; Du, G. Tannin-Furanic Foams Modified by Soybean Protein Isolate (SPI) and Industrial Lignin Substituting Formaldehyde Addition. *Ind. Crops Prod.* **2021**, *168*, 113607. [[CrossRef](#)]
29. Missio, A.L.; Delucis, R.A.; Otoni, C.G.; de Cademartori, P.H.G.; Coldebella, R.; Aramburu, A.B.; Mattos, B.D.; Rodrigues, M.B.B.; Lunkes, N.; Gatto, D.A.; et al. Thermally Resistant, Self-Extinguishing Thermoplastic Composites Enabled by Tannin-Based Carbonaceous Particulate. *Polymers* **2022**, *14*, 3743. [[CrossRef](#)]
30. Li, J.; Liao, J.; Essawy, H.; Zhang, J.; Li, T.; Wu, Z.; Du, G.; Zhou, X. Preparation and Characterization of Novel Cellular/Nonporous Foam Structures Derived from Tannin Furanic Resin. *Ind. Crops Prod.* **2021**, *162*, 113264. [[CrossRef](#)]
31. Li, J.; Zhang, A.; Zhang, S.; Gao, Q.; Zhang, W.; Li, J. Larch Tannin-Based Rigid Phenolic Foam with High Compressive Strength, Low Friability, and Low Thermal Conductivity Reinforced by Cork Powder. *Compos. Part B Eng.* **2019**, *156*, 368–377. [[CrossRef](#)]
32. Tondi, G.; Pizzi, A. Tannin-Based Rigid Foams: Characterization and Modification. *Ind. Crops Prod.* **2009**, *29*, 356–363. [[CrossRef](#)]
33. Tondi, G.; Zhao, W.; Pizzi, A.; Du, G.; Fierro, V.; Celzard, A. Tannin-Based Rigid Foams: A Survey of Chemical and Physical Properties. *Bioresour. Technol.* **2009**, *100*, 5162–5169. [[CrossRef](#)] [[PubMed](#)]
34. Westhoff, D.; Skibinski, J. Investigation of the Relationship between Morphology and Permeability for Open-Cell Foams Using Virtual Materials Testing. *Mater. Des.* **2018**, *147*, 1–10. [[CrossRef](#)]
35. Lacoste, C.; Basso, M.C.; Pizzi, A.; Celzard, A.; Laborie, M.-P. Natural Albumin/Tannin Cellular Foams. *Ind. Crops Prod.* **2015**, *73*, 41–48. [[CrossRef](#)]
36. Delucis, R.d.A.; Magalhães, W.L.E.; Petzhold, C.L.; Amico, S.C. Thermal and Combustion Features of Rigid Polyurethane Biofoams Filled with Four Forest-Based Wastes. *Polym. Compos.* **2018**, *39*, E1770–E1777. [[CrossRef](#)]
37. Basso, M.C.; Lagel, M.-C.; Pizzi, A.; Celzard, A.; Abdalla, S. First Tools for Tannin-Furanic Foams Design. *BioResources* **2015**, *10*, 5233–5241. [[CrossRef](#)]

38. Galvão, Á.C.P.; Farias, A.C.M.; Mendes, J.U.d.L. Obtaining and Characterization of the Rigid Polyurethane (PUR) Filled with Soda–Lime Glass Powder (GP) from Waste of Lapping. *HOLOS* **2015**, *5*, 104–118. [[CrossRef](#)]
39. Tondi, G.; Link, M.; Kolbitsch, C.; Petutschnigg, A. Infrared-Catalyzed Synthesis of Tannin-Furanic Foams. *BioResources* **2014**, *9*, 984–993. [[CrossRef](#)]
40. Soltanpour, Z.; Mohammadian, Y.; Fakhri, Y. The Exposure to Formaldehyde in Industries and Health Care Centers: A Systematic Review and Probabilistic Health Risk Assessment. *Environ. Res.* **2022**, *204*, 112094. [[CrossRef](#)]
41. Basso, M.C.; Giovando, S.; Pizzi, A.; Celzard, A.; Fierro, V. Tannin/Furanic Foams without Blowing Agents and Formaldehyde. *Ind. Crops Prod.* **2013**, *49*, 17–22. [[CrossRef](#)]
42. Liu, B.; Zhou, Y.; Essawy, H.; Feng, S.; Li, X.; Liao, J.; Zhou, X.; Zhang, J.; Xie, S. Formaldehyde Free Renewable Thermosetting Foam Based on Biomass Tannin with a Lignin Additive. *J. Renew. Mater.* **2022**, *10*, 3009–3024. [[CrossRef](#)]
43. Link, M.; Kolbitsch, C.; Tondi, G.; Ebner, M.; Wieland, S.; Petutschnigg, A. Formaldehyde-Free Tannin-Based Foams and Their Use as Lightweight Panels. *BioResources* **2011**, *6*, 4218–4228. [[CrossRef](#)]
44. Jin, F.-L.; Zhao, M.; Park, M.; Park, S.-J. Recent Trends of Foaming in Polymer Processing: A Review. *Polymers* **2019**, *11*, 953. [[CrossRef](#)] [[PubMed](#)]
45. Khiari, R.; Baaka, N.; Ammar, M.; Saad, M.K. Properties of Tannin-Glyoxal Resins Prepared from Lyophilized and Condensed Tannin. *J. Text. Eng. Fash. Technol.* **2017**, *3*, 705–711. [[CrossRef](#)]
46. Gaugler, M.; Grigsby, W.J. Thermal Degradation of Condensed Tannins from Radiata Pine Bark. *J. Wood Chem. Technol.* **2009**, *29*, 305–321. [[CrossRef](#)]
47. Chen, X.; Xi, X.; Pizzi, A.; Fredon, E.; Zhou, X.; Li, J.; Gerardin, C.; Du, G. Preparation and Characterization of Condensed Tannin Non-Isocyanate Polyurethane (NIPU) Rigid Foams by Ambient Temperature Blowing. *Polymers* **2020**, *12*, 750. [[CrossRef](#)] [[PubMed](#)]
48. Zhang, A.; Li, J.; Zhang, S.; Mu, Y.; Zhang, W.; Li, J. Characterization and Acid-Catalyzed Depolymerization of Condensed Tannins Derived from Larch Bark. *RSC Adv.* **2017**, *7*, 35135–35146. [[CrossRef](#)]
49. Duval, A.; Avérous, L. Characterization and Physicochemical Properties of Condensed Tannins from Acacia Catechu. *J. Agric. Food Chem.* **2016**, *64*, 1751–1760. [[CrossRef](#)]
50. Lee, S.H.; Lee, S.G.; Lee, J.S.; Ma, B.C. Understanding the Flame Retardant Mechanism of Intumescent Flame Retardant on Improving the Fire Safety of Rigid Polyurethane Foam. *Polymers* **2022**, *14*, 4904. [[CrossRef](#)]
51. Zhu, H.; Wang, Z.; Liu, N.; Gao, W.; Xie, X.; Huang, M. Thermal Decomposition of Flexible Polyurethane Foam under Nitrogen and Air Atmospheres: Thermogravimetric Analysis by ETp Method. *Thermochim. Acta* **2023**, *727*, 179572. [[CrossRef](#)]
52. Yadav, A.; de Souza, F.M.; Dawsey, T.; Gupta, R.K. Recent Advancements in Flame-Retardant Polyurethane Foams: A Review. *Ind. Eng. Chem. Res.* **2022**, *61*, 15046–15065. [[CrossRef](#)]
53. Muhammed Raji, A.; Hambali, H.U.; Khan, Z.I.; Binti Mohamad, Z.; Azman, H.; Ogabi, R. Emerging Trends in Flame Retardancy of Rigid Polyurethane Foam and Its Composites: A Review. *J. Cell. Plast.* **2023**, *59*, 65–122. [[CrossRef](#)]
54. Kolbitsch, C.; Link, M.; Petutschnigg, A.; Wieland, S.; Tondi, G. Microwave Produced Tannin-Furanic Foams. *J. Mater. Sci. Res.* **2012**, *1*, 84. [[CrossRef](#)]
55. Pikhurov, D.V.; Sakhatskii, A.S.; Zuev, V.V. Rigid Polyurethane Foams with Infused Hydrophilic/Hydrophobic Nanoparticles: Relationship between Cellular Structure and Physical Properties. *Eur. Polym. J.* **2018**, *99*, 403–414. [[CrossRef](#)]
56. Zhang, J.; Hori, N.; Takemura, A. Optimization of Preparation Process to Produce Polyurethane Foam Made by Oilseed Rape Straw Based Polyol. *Polym. Degrad. Stab.* **2019**, *166*, 31–39. [[CrossRef](#)]
57. Tita, S.P.S.; de Paiva, J.M.F.; Frollini, E. Impact Strength and Other Properties of Lignocellulosic Composites: Phenolic Thermoset Matrices Reinforced with Sugarcane Bagasse Fibers. *Polímeros* **2002**, *12*, 228–239. [[CrossRef](#)]
58. Brazilian Association of the Wood Panel Industry. Program Sector of the Quality of Medium Density Particleboard (MDP) and Medium Density Fiberboard (MDF)—Sector Report No. 044. Available online: <https://pbqp-h.mdr.gov.br/wp-content/uploads/2021/09/RS-044.pdf> (accessed on 15 September 2023).
59. Zhao, W.; Pizzi, A.; Fierro, V.; Du, G.; Celzard, A. Effect of Composition and Processing Parameters on the Characteristics of Tannin-Based Rigid Foams. Part I: Cell Structure. *Mater. Chem. Phys.* **2010**, *122*, 175–182. [[CrossRef](#)]

**Disclaimer/Publisher’s Note:** The statements, opinions and data contained in all publications are solely those of the individual author(s) and contributor(s) and not of MDPI and/or the editor(s). MDPI and/or the editor(s) disclaim responsibility for any injury to people or property resulting from any ideas, methods, instructions or products referred to in the content.